Збірник наукових праць. Галузеве машинобудування, будівництво
Academic journal. Industrial Machine Building, Civil Engineering
http://journals.nupp.edu.ua/znp
https://doi.org/10.26906/znp.2026.66.4356

UDC 625.745.22:627.837

Artur Onyshchenko
National Transport University
https://orcid.org/0000-0002-1040-4530

Yana Dukhnenko *
National Transport University
https://orcid.org/0009-0007-8742-7718

Simulation Models of the Lower Tailwater Structure of Road Culverts

Abstract. The problem of excess kinetic energy dissipation in the lower tailwater of road culverts [15] and drainage structures is considered. The paper presents an analysis of the operating conditions of active-type energy dissipators based on a pressureless energy-dissipating diffuser concept. Three fundamental types of dissipator action on the flow — reactive, dissipative, and distributive — are reviewed as the theoretical framework [1–3]. The factors determining the effectiveness of a spatial energy-dissipating diffuser are identified: the flow rate parameter, the relative width of the discharge channel, the throat opening, the wall installation angle, and the wall height. A D-optimal experimental design was implemented to obtain statistical models of the diffuser operation. Comparative hydraulic model tests of the conventional retaining-wall dissipator and the energy-dissipating diffuser were conducted under varying flow discharges and tailwater submergence conditions. Results show that the relative near-bed velocity downstream of the diffuser is approximately three times lower than that downstream of the conventional retaining-wall dissipator.

Keywords: energy dissipator, culvert, hydraulic jump, energy-dissipating diffuser, tailwater, kinetic energy, road drainage

*Corresponding author E-mail: yana.duhnenko@gmail.com

Received: 05.03.2026 Accepted: 01.05.2026 Published: 31.05.2026

Introduction.

To ensure optimal flow connection and reduce the length of the protection zone in the lower tailwater of culverts [15] and drainage structures, excess kinetic energy dissipators are installed. Studies of energy dissipator hydraulics [1–3] identify three fundamental types of dissipator action on the flow: reactive, dissipative, and distributive.

The ***reactive*** action consists of the dissipator protruding above the channel floor and acting against the flow on the apron. This leads to the formation (or submergence) of a hydraulic jump at depths smaller than required by the standard jump equation.

The ***dissipative*** action refers to the influence the dissipator exerts on the intensity of the energy dissipation process. Slit-wall type dissipators, high-roughness rib-type elements, and similar structures belong to this category.

In the ***distributive*** action, the energy dissipator deflects the high-velocity transit jet toward the free surface, converting the flow from the bottom to the surface mode with a sharp reduction in near-bottom velocities, thereby significantly reducing the scour potential downstream.

In practice, the most common dissipators in land reclamation and road construction [7] are solid or slit retaining walls, combinations of two or more walls, high-roughness surfaces, stilling basins formed by lowering the bed level, etc. [2–6]. All can be attributed to one of these three fundamental types.

Problem statement. None of the known structural solutions fully satisfies all the requirements imposed on the lower tailwater of road drainage structures, so designers are forced to solve “compromise” problems [12] – enhancing certain properties at the expense of others. A principally new structural design is therefore required that addresses energy dissipation while meeting the specific service conditions of road culvert tailwaters.

Main material and results. An earlier study [4] proposed narrowing the cross-section of a turbulent flow using high walls set at an angle to the flow – the “pressureless energy-dissipating diffuser” (Fig. 1). Theoretical and experimental research demonstrated that, under plane-flow conditions, this design ensures a high degree of energy dissipation under significant

water-level fluctuations in the lower tailwater while simultaneously allowing floating objects to pass. The extension of this concept to spatial-flow conditions ($\beta > 1$) required further development and is addressed in the present paper.

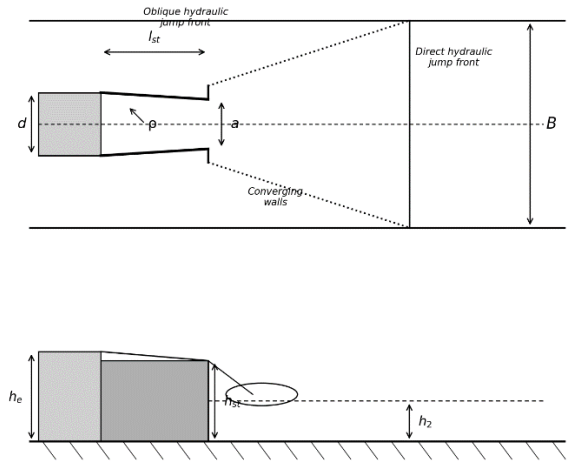

Figure 1 – Design diagram of the energy-dissipating diffuser

For the spatial-flow case, the diffuser geometry was redesigned. The original configuration caused an unacceptable concentration of unit discharges along the channel axis at shallow tailwater depths, requiring bed protection over a large downstream distance. To achieve a uniform transverse distribution of unit discharges q, mean velocities u, depths h, and turbulence intensity parameters M, the height of the converging walls was reduced, enabling partial surface overflow and a more uniform velocity distribution across the channel width.

The effectiveness of the energy-dissipating diffuser is governed by the following factors: flow discharge Q; wall height h_{st}; wall installation angle α; wall length l_{st}; relative channel width $\beta = B/b$; throat opening width a; and the longitudinal position of the walls in the channel [8].

Wall installation angle. For the plane-flow case, it was established [4] that the wall angle α may range from αmin to 90°, where αmin is the reflection angle of the outermost streamline of the expanding supercritical flow from the lateral wall. At $\alpha > \alpha_{min}$, dynamic loads on the walls increase sharply, so $\alpha = \alpha_{min}$ is recommended for design purposes. For the case of sudden channel expansion, the wall angle must be set equal to the angle of convergence of the oblique hydraulic jumps formed at the channel transition.

Preliminary analysis established that: (a) the inlet headwall has virtually no effect on the hydraulic characteristics of the free-spreading zone; (b) for pipe lengths exceeding 7d, the pipe length has a negligible influence on the spreading pattern. A pipe length of 9d and a flared inlet head were therefore adopted in all subsequent experiments, removing these parameters from the factor space. The Froude number F_r, which is a two-valued function of discharge for circular pipes, was replaced by the flow rate parameter Π_q, a single-valued, directly controllable variable.

The five primary factors governing the operation of the pressureless energy-dissipating diffuser were identified as: (1) flow rate parameter Π_q; (2) relative channel expansion $\beta = B/b$; (3) relative throat opening a/d; (4) relative wall angle α/α_{pr}; and (5) relative wall height h_{st}/d. Research was conducted for the most demanding operational case: maximum spreading-zone dimensions and maximum flow velocities. The three dimensional factors were non-dimensionalised using the pipe diameter d and the limiting angle αpr corresponding to complete flow spreading. The wall position was fixed at the full-spreading cross-section L_{pt} and was not treated as an independent variable, as it correlates with β and Π_q.

Additional experiments were conducted to determine αpr and L_{pt}/d as functions of relative expansion. Results are given in Table 1.

Table 1 – Effect of relative channel expansion on α_{pr} and L_{pt}/d

β_{pr}	3.0	4.0	5.0	6.0	7.0	8.0
α_{pr}, °	15.2	12.3	12.9	13.9	14.8	16.0
L_{ps}/d	1.04	1.30	1.76	2.15	2.63	3.16

The flow rate parameter K_{nq} was defined as the ratio $K_{nq}=exp(\Pi_q)/exp(\Pi_{qmin})$, where Π_{qmin} is the boundary value at which fully-developed oblique hydraulic jumps first appear. Its variation range and the corresponding Π_q values for three channel widths are given in Table 2.

Table 2 – Variation range of parameter K_{nq} and corresponding flow rate parameter Π_q

K_{nq}	Flow rate parameter Π_q		
	$\beta = 3.0$	$\beta = 5.5$	$\beta = 8.0$
2.234	0.904	1.060	1.250
1.617	0.508	0.740	0.926
1.000	0.100	0.258	0.446

The factor variation intervals used in the experiment are summarised in Table 3.

Table 3 – Factor levels and coded values

Factors	Factor levels			
Natural	Code	−1	0	+1
K_{nq}	X_1	1.000	1.617	2.234
β	X_2	3.0	5.5	8.0
a/d	X_3	0	0.5	1.0
α/α_{pr}	X_4	1	2	3
h_{st}/d	X_5	0.2	0.5	0.8

Optimisation parameters. To characterise dissipator effectiveness as an energy dissipation device, the following parameter was adopted:

$$Y_1 = (W - W_p) / W, \quad (1)$$

where W is the required bed protection area for free spreading of the supercritical flow without the diffuser, and W_p is the protection area with the diffuser installed. The larger Y_1, the greater the reduction in required protection length. To verify the objectivity of Y_1, additional tests on a mobile-bed model (3 m long, 0.5 m deep) established a close relationship between Y_1 and the relative scour volume:

$$Y_2 / Y_1 = (V / V_p)^{2.5}, \quad (2)$$

where V and V_p are scour volumes without and with the diffuser, respectively. This confirmed the validity of Y_1 as the primary optimisation criterion, allowing all subsequent experiments to be conducted on fixed-bed models.

The second optimisation parameter, which characterises the diffuser as a flow-distribution device, is defined as:

$$Y_2 = sign \cdot \Sigma[(u_a - \bar{u}_{ai})^2 / (U_e (n - 1))]^{1/2}, \quad (3)$$

where u_a is the actual mean near-bed velocity in the measurement cross-section; U_e is the mean outflow velocity at the pipe exit; n is the number of measurements across the section; and sign assigns a positive or negative value depending on whether near-bed velocities are higher along the axis or near the channel wall ("+" when axis velocity exceeds wall velocity, "–" otherwise). The reference cross-section for Y_2 was taken at a distance of B from the end of the diffuser.

Experimental design. An approximate D-optimal experimental design was used to obtain polynomial regression models [14]. Because a preliminary analysis suggested that the response surface might exhibit significant nonlinearity, a five-factor B5 fractional factorial plan with three centre-point replicates (29 experiment runs) was adopted as the starting design. According to the statistical assessment of Hartmann et al. [13], this plan combines near-optimal D- and G-optimality properties.

Table 4 – Initial B5 fractional factorial plan (coded factor values)

№№	X_1	X_2	X_3	X_4	X_5	№№	X_1	X_2	X_3	X_4	X_5
1	-1	-1	-1	-1	+1	16	+1	+1	+1	+1	+1
2	+1	-1	-1	-1	-1	17	-1	0	0	0	0
3	-1	+1	-1	-1	-1	18	+1	0	0	0	0
4	+1	+1	-1	-1	+1	19	0	-1	0	0	0
5	-1	-1	+1	-1	-1	20	0	+1	0	0	0
6	+1	-1	+1	-1	+1	21	0	0	-1	0	0
7	-1	+1	+1	-1	+1	22	0	0	+1	0	0
8	+1	+1	+1	-1	-1	23	0	0	0	-1	0
9	-1	-1	-1	+1	-1	24	0	0	0	+1	0
10	+1	-1	-1	+1	+1	25	0	0	0	0	-1
11	-1	+1	-1	+1	+1	26	0	0	0	0	+1
12	+1	+1	-1	+1	-1	27	0	0	0	0	0
13	-1	-1	+1	+1	+1	28	0	0	0	0	0
14	+1	-1	+1	+1	-1	29	0	0	0	0	0
15	-1	+1	+1	+1	-1						

The experimental values of the optimisation parameters obtained from the B5 plan are given in Table 5.

Statistical model selection. Initial fitting of a standard second-order polynomial to the B5 plan results showed that the model was inadequate: the variance of adequacy S^2_a exceeded the variance of reproducibility [11] S^2_e by a factor of approximately 250, indicating that the response surface contains significant higher-order effects.

Table 5 – Experimental values of optimisation parameters (B5 plan)

№№	Y_1	Y_2	№№	Y_1	Y_2	№№	Y_1	Y_2
1	2.752	0.0052	11	2.366	-0.0279	21	1.951	0.0287
2	2.629	0.0372	12	1.092	0.1317	22	1.830	0.0202
3	1.138	0.0096	13	1.232	0.1174	23	1.839	0.0042
4	1.153	-0.0026	14	1.665	0.1121	24	1.485	0.1731
5	2.113	0.0216	15	1.237	0.0326	25	1.414	0.0622
6	1.863	0.0353	16	0.946	0.1102	26	1.397	0.0716
7	0.932	0.0033	17	1.175	0.0604	27	1.707	0.0359
8	0.944	0.0606	18	1.545	0.0164	28	1.732	0.0372
9	1.868	0.0363	19	2.415	0.0952	29	1.682	0.0428
10	4.176	-0.0459	20	1.296	0.0126			

Following sequential augmentation of the experimental plan with additional points at which the prediction error was highest, incomplete cubic interaction terms of the form $B_i X_i^2 X_j$ and triple interactions were progressively added to the model. A statistically adequate model was obtained:

$$\begin{aligned} Y_1 = {} & 1.6434 + 0.2010X_1 - 0.5376X_2 - \\ & 0.0573X_3 - 0.1627X_4 + 0.0082X_5 + \\ & + 0.0791X_1X_2 - 0.0624X_1X_3 - 0.0940X_1X_4 + \\ & 0.0558X_1X_5 + \\ & + 0.1790X_2X_3 + 0.1164X_2X_4 - 0.1494X_2X_5 - \\ & 0.4194X_3X_4 - 0.2983X_3X_5 + \\ & + 0.1865X_4X_5 - 0.2391X_1^2 + 0.2611X_2^2 + \\ & 0.2833X_3^2 - 0.1951X_5^2 + \\ & + 0.2275X_1^2X_4 + 0.3316X_4^2X_3 + 0.1611X_4^2X_5 \\ & - 0.1482X_5^2X_1 + \\ & + 0.2371X_1X_2X_5 + 0.1020X_1X_3X_4 - \\ & - 0.2459X_3X_4X_5. \end{aligned} \quad (4)$$

The adequacy check gave $F = S^2_a / S^2_e = 0.01992 / 0.00985 = 2.02$, which is less than the tabulated value $F(6; 32) = 2.4$. The model therefore does not contradict the experimental data.

Flow kinematics downstream of the diffuser. An analysis of the influence of each factor on the near-bed mean velocity profile in the discharge channel (Fig. 2) yielded the following main findings. Increasing the flow rate parameter from $X_1 = -1$ to $X_1 = +1$ substantially changes the near-bed velocity distribution: in the flow-connection zone ($x = 0.6–1.2$), relative near-bed velocities at minimum discharge are 1.5–2.0 times higher than at maximum discharge, while beyond $x = 1.2$ the pattern reverses and velocities at minimum discharge drop to roughly one-third of those at maximum.

Increasing the relative channel expansion β from 3 ($X_2 = -1$) to 8 ($X_2 = +1$) reduces near-bed mean velocities throughout the connection reach: the larger the relative expansion, the lower the near-bed mean velocity at any given cross-section. The relative throat opening a/d (factor X_3) has only a minor influence on the mean velocity profile, except that a fully closed

throat ($X_3 = -1$) produces a slight non-monotonic velocity distribution in the zone x = 0.6–0.9, attributed to overflow over the walls when no throat gap exists.

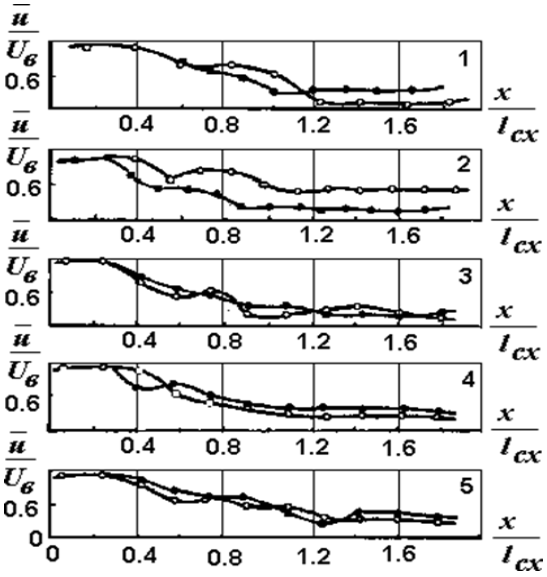

Figure 2 – Influence of governing factors on the near-bed mean velocity profile (X = 0 baseline and ±1 variants)

Increasing the relative wall angle α/αpr (factor X_4) raises the near-bed mean velocity by 20–30 % and makes the profile monotonically decreasing beyond x > 0.6. Reducing the wall height (factor X_5) produces a moderate decrease in mean velocities due to more uniform transverse discharge distribution resulting from overflow over the shorter walls.

Interpretation of results. Comparative hydraulic model tests of the conventional retaining-wall dissipator [2, 5] and the energy-dissipating diffuser were conducted for two test programmes: (i) varying discharge over the range 0.6 < H/d < 1.6 with no tailwater submergence; (ii) varying tailwater depth at constant head H/d = 1.1. Diffuser dimensions were selected at H/d = 1.1 using the design relationships derived from the statistical model.

Under varying discharge without submergence, the conventional dissipator produced intense fountain jets at each wall and a supercritical regime with repeated oblique wave crests along the entire discharge channel at all tested heads. A direct hydraulic jump appeared in the channel only after substantial tailwater rise. By contrast, the diffuser basin exhibited a subcritical flow regime at all discharge levels: a transit jet and a well-developed surface roller were visible inside the basin, with fine ripples on the water surface confirming subcritical conditions immediately downstream of the walls at every tested head.

As discharge increased (H/d from 1.0 to 1.4), the transit jet in the diffuser basin progressively widened. At the highest tested head, a “bridge-type” hydraulic jump formed — a combination of one direct hydraulic jump at the end of the spreading zone flanked by two symmetrical oblique hydraulic jumps oriented nearly parallel to the converging walls. This stable three-jump configuration proved to be the principal energy-dissipation mechanism of the diffuser at high discharges.

The near-bed relative velocity downstream of the diffuser beyond the spreading zone was approximately three times lower than that downstream of the conventional design (Fig. 3), confirming the qualitative flow observations.

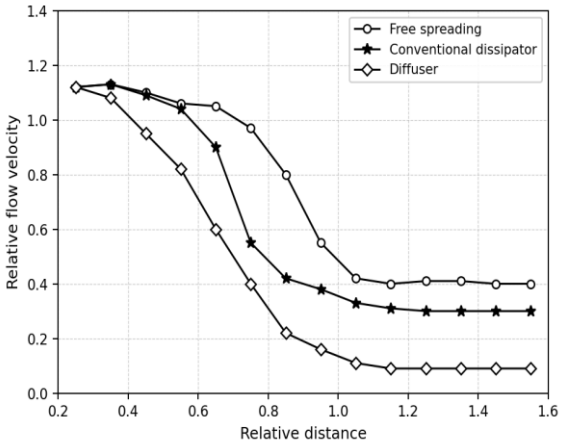

Figure 3 – Comparison of near-bed velocity profiles: energy-dissipating diffuser vs. conventional dissipator

Conclusions.

The development of active-type dissipators for two-dimensional turbulent flows, extending an established pressureless diffuser concept [4] from one-dimensional to spatial-flow conditions, proved highly promising.

Based on hydraulic research of the two-dimensional turbulent flow spreading zone, it was established that an active-type dissipator must include two flow-deflecting walls positioned at the cross-section of complete spreading along the lines of convergence of oblique hydraulic jumps. Wall height must ensure the possibility of surface overflow.

Statistical models obtained from an approximate D-optimal experimental design allow selecting optimal ratios of structural elements to form a discharge channel flow with specified hydraulic characteristics, ensuring maximum energy dissipation with maximum uniformity of the plan velocity distribution.

The “bridge-type” hydraulic jump is an effective dissipator of excess kinetic energy of a two-dimensional freely spreading turbulent flow. The dissipator structure — two flow-guiding walls set along the oblique hydraulic jump fronts allowing surface overflow — stabilises the direct hydraulic jump and renders it practically independent of discharge magnitude and tailwater level fluctuations.

References

1. Hager, W. H. (1992). Energy dissipators and hydraulic jump. *Kluwer Academic Publishers*. https://doi.org/10.1007/978-94-015-8048-9

1. Hager, W. H. (1992). Energy dissipators and hydraulic jump. *Kluwer Academic Publishers*. https://doi.org/10.1007/978-94-015-8048-9

2. Peterka, A. J. (1984). *Hydraulic design of stilling basins and energy dissipators* (Engineering Monograph No. 25). US Bureau of Reclamation.

3. Онищенко А. М., Ковальчук В. В., Гаркуша М. В., Цивін М. Н., Карнаков І. А., Мошківський Р. В. *Забезпечення надійності та довговічності гідротехнічних споруд транспортного будівництва з дорожніх водопропускних труб в умовах експлуатації: монографія*. Київ : «Видавництво Людмила», 2023. 179 с. https://doi.org/10.32751/Mono_Zabez2023

4. Онищенко А. М., Гаркуша М. В., Клименко М. І. Аналіз конструктивних заходів з укріплення нижніх б'єфів гідротехнічних споруд у транспортному будівництві з дорожніх водопропускних труб. *Дороги і мости*. 2022. Вип. 26. С. 215–227. https://doi.org/10.36100/dorogimosti2022.26.215

5. Цивін М. Н., Ткаченко Н. І. Оптимальна конструкція кріплення нижнього б'єфу водопропускних споруд систем лиманного зрошення. *Гідромеліорація та гідротехнічне будівництво*. 1988. Вип. 16. С. 38–43.

6. Chanson, H. (2009). Turbulent air-water flows in hydraulic structures: dynamic similarity and scale effects. *Environmental Fluid Mechanics*, 9(2), 125–142. https://doi.org/10.1007/s10652-008-9078-3

7. Onyshchenko, A., Ostroverkh, B., Potapenko, L., Kovalchuk, V., Zdolnyk, O., & Pentsak, A. (2024). Devising a procedure for integrated modeling of riverbed shape in the area of bridge crossing in order to avoid dangerous washing erosion. *Eastern-European Journal of Enterprise Technologies*, 1(1(127)), 23–32. https://doi.org/10.15587/1729-4061.2024.298675

8. Onyshchenko, A., Kovalchuk, V., Voskoboinick, V., Voskobiinyk, A., Aksonov, S., Trudenko, D., & Hrevtsov, S. (2024). Establishing patterns of change in the coefficients of reflection, transmission, and dissipation of wave energy depending on parameters of a permeable vertical wall. *Eastern-European Journal of Enterprise Technologies*, 4(5(130)), 45–56. https://doi.org/10.15587/1729-4061.2024.309969

9. Kovalchuk, V., Sysyn, M., Hnativ, Y., Onyshchenko, A., Koval, M., Tiutkin, O., & Parneta, M. (2021). Restoration of the bearing capacity of damaged transport constructions made of corrugated metal structures. *The Baltic Journal of Road and Bridge Engineering*, 16(2), 90–109.

10. Kovalchuk, V., Karnakov, I., Onyshchenko, A., Petrenko, O., & Boikiv, R. (2023). Assessing the stresses and magnitude of plastic hinge in a tunnel conduit made of precast metal corrugated structures taking into account the soil backfill parameters. *Eastern-European Journal of Enterprise Technologies*, 4/7(124), 43–53. https://doi.org/10.15587/1729-4061.2023.285893

11. Цівін, М. М., & Чернишевська, Л. Ю. (2005). Статистичний підхід до оцінки ущільнення різних типів ґрунтів. Вісник аграрної науки, (Ювілейний випуск), 58–61.

12. Цівін, М. М. (2004). До проблеми оптимізації протиерозійних гідротехнічних споруд: постановка задачі. *Меліорація і водне господарство*, 91, 234–244.

13. Hartmann, K., Lezki, E., & Schäfer, W. (1974). Statistische Versuchsplanung und -auswertung in der Stoffwirtschaft. Deutscher Verlag für Grundstoffindustrie.

14. Forsythe, G. E., Malcolm, M. A., & Moler, C. B. (1977). Computer methods for mathematical computations. Prentice-Hall.

15. Canadian Standards Association. (2014). *Corrugated steel pipe products* (CAN/CSA Standard G401-14). CSA Group.

2. Peterka, A. J. (1984). *Hydraulic design of stilling basins and energy dissipators* (Engineering Monograph No. 25). US Bureau of Reclamation.

3. Onyshchenko, A. M., Kovalchuk, V. V., Garkusha, M. V., Tsivin, M. N., Karnakov, I. A., & Moshkovsky, R. V. (2023). Ensuring the reliability and durability of hydraulic structures in transport construction using road culverts under operating conditions: monograph. Lyudmila Publishing House. https://doi.org/10.32751/Mono_Zabez2023

4. Onyshchenko, A. M., Harkusha, M. V., & Klymenko, M. I. (2022). Analysis of constructive measures for strengthening the downstream channels of hydraulic structures in transport construction using road culverts. Dorohy i mosty (Roads and Bridges), 26, 215–227. https://doi.org/10.36100/dorogimosti2022.26.215

5. Tsivin, M. N., & Tkachenko, N. I. (1988). Optimalna konstruktsiia kriplennia nyzhnoho b'iefu vodopropusknykh sporud lyman_noho zroshennia Hidromelioratsiia ta hidrotekhnichne budivnytstvo, 16, 38–43.

6. Chanson, H. (2009). Turbulent air-water flows in hydraulic structures: dynamic similarity and scale effects. *Environmental Fluid Mechanics*, 9(2), 125–142. https://doi.org/10.1007/s10652-008-9078-3

7. Onyshchenko, A., Ostroverkh, B., Potapenko, L., Kovalchuk, V., Zdolnyk, O., & Pentsak, A. (2024). Devising a procedure for integrated modeling of riverbed shape in the area of bridge crossing in order to avoid dangerous washing erosion. *Eastern-European Journal of Enterprise Technologies*, 1(1(127)), 23–32. https://doi.org/10.15587/1729-4061.2024.298675

8. Onyshchenko, A., Kovalchuk, V., Voskoboinick, V., Voskobiinyk, A., Aksonov, S., Trudenko, D., & Hrevtsov, S. (2024). Establishing patterns of change in the coefficients of reflection, transmission, and dissipation of wave energy depending on parameters of a permeable vertical wall. *Eastern-European Journal of Enterprise Technologies*, 4(5(130)), 45–56. https://doi.org/10.15587/1729-4061.2024.309969

9. Kovalchuk, V., Sysyn, M., Hnativ, Y., Onyshchenko, A., Koval, M., Tiutkin, O., & Parneta, M. (2021). Restoration of the bearing capacity of damaged transport constructions made of corrugated metal structures. *The Baltic Journal of Road and Bridge Engineering*, 16(2), 90–109.

10. Kovalchuk, V., Karnakov, I., Onyshchenko, A., Petrenko, O., & Boikiv, R. (2023). Assessing the stresses and magnitude of plastic hinge in a tunnel conduit made of precast metal corrugated structures taking into account the soil backfill parameters. *Eastern-European Journal of Enterprise Technologies*, 4/7(124), 43–53. https://doi.org/10.15587/1729-4061.2023.285893

11. Tsivin, M. N., & Chernyshevska, L. Yu. (2005). Statistical approach to assessing the compaction of different soil types. *Bulletin of Agricultural Science*, (Jubilee Issue), 58–61.

12. Tsivin, M. N. (2004). On the problem of optimization of anti-erosion hydraulic structures: Problem statement. *Land Reclamation and Water Management*, 91, 234–244.

13. Hartmann, K., Lezki, E., & Schäfer, W. (1974). Statistische Versuchsplanung und -auswertung in der Stoffwirtschaft. Deutscher Verlag für Grundstoffindustrie.

14. Forsythe, G. E., Malcolm, M. A., & Moler, C. B. (1977). Computer methods for mathematical computations. Prentice-Hall.

15. Canadian Standards Association. (2014). *Corrugated steel pipe products* (CAN/CSA Standard G401-14). CSA Group.

Онищенко А.М.
Національний транспортний університет
https://orcid.org/0000-0002-1040-4530

Духненко Я.С. *
Національний транспортний університет
https://orcid.org/0009-0007-8742-7718

Імітаційні моделі роботи конструкції нижнього б'єфу дорожніх водопропускних споруд

Аннотація. Розглядається проблема гасіння надлишкової кінетичної енергії потоку в нижньому б'єфі дорожніх водопропускних і водовідвідних споруд. Наведено аналіз роботи гасителів енергії активного типу на основі концепції безтискового енергогасячого дифузора. Розглянуто три основні типи впливу гасителя на потік [1–3, 11–12]. Визначено фактори, що визначають ефективність роботи просторового енергогасачого дифузора: параметр витрати, відносна ширина відвідного русла, ширина горловини, кут встановлення стінок та їх висота. Для отримання статистичних моделей роботи дифузора реалізовано наближений D-оптимальний план експерименту. Проведено порівняльні гідравлічні модельні дослідження стандартного гасника та енергогасачого дифузора за різних витрат та ступенів підтоплення нижнього б'єфу. Встановлено, що відносна придонна швидкість за дифузором поза зоною розтікання майже втричі менша, ніж за стандартним гасником.

Ключові слова: гаситель енергії, водопропускна споруда, гідравлічний стрибок, енергогасачий дифузор, нижній б'єф, кінетична енергія, дорожнє водовідведення

*Адреса для листування E-mail: yana.duhnenko@gmail.com

Надіслано до редакції:	05.03.2026	Прийнято до друку після рецензування:	01.05.2026	Опубліковано (оприлюднено):	31.05.2026

Suggested Citation:	
APA style	Onyshchenko, A., & Dukhnenko, Ya. (2026). Simulation Models of the Lower Tailwater Structure of Road Culverts. *Academic Journal Industrial Machine Building Civil Engineering*, *1*(66), 35–40. https://doi.org/10.26906/znp.2026.66.4356
DSTU style	Onyshchenko A., Dukhnenko Ya. Simulation Models of the Lower Tailwater Structure of Road Culverts. *Academic journal. Industrial Machine Building, Civil Engineering*. 2026. Vol. 66, iss. 1. P. 35–40. URL: https://doi.org/10.26906/znp.2026.66.4356